Experimental Study on Heat Transfer and Friction Factor Characteristics of Single Layer Graphene Based DI-water Nanofluid in a Circular Tube under Laminar Flow and Different Heat Fluxes as Boundary Conditions

Prof. Dr. Najdat N. Abdullah
Department of Mechanical Engineering
University of Baghdad
E mail: najdat_abdulla@yahoo.co.uk

Hussein A. Ibrahim
Department of Mechanical Engineering
University of Baghdad
E mail: hussain1983ali@gmail.com

ABSTRACT

An experimental study was performed to estimate the forced convection heat transfer performance and the pressure drop of a single layer graphene (GNPs) based DI-water nanofluid in a circular tube under a laminar flow and a uniform heat flux boundary conditions. The viscosity and thermal conductivity of nanofluid at weight concentrations of (0.1 to 1 wt%) were measured. The effects of the velocity of flow, heat flux and nanoparticle weight concentrations on the enhancement of the heat transfer are examined. The Nusselt number of the GNPs nanofluid was enhanced as the heat flux and the velocity of flow rate increased, and the maximum Nusselt number ratio ($Nu_{nanofluid}/Nu_{base\ fluid}$) and thermal performance factor was (1.45) and (1.24) respectively, by using (1wt%) concentration and $q=6104W/m^2$ heat flux. Finally, an analysis of the thermal performance factor shows that the GNPs nanofluids could work as a good alternative conventional working fluid in thermal heat transfer applications.

Key words: convective heat transfer, graphene nanofluid, laminar flow, pressure drop, performance factor

دراسة تجريبية على خصائص انتقال الحرارة ومعامل الاحتكاك لمائع نانوي احادي الطبقة (كرافين-ماء) في انبوب دائري تحت الجريان الانسيابي واحمال حرارية مختلفة كشروط حدودية

أ.د. نجدت نشأت عبدالله
قسم الهندسة الميكانيكية
جامعة بغداد

حسين علاوي ابراهيم
قسم الهندسة الميكانيكية
جامعة بغداد

تم اجراء دراسة تجريبية لحساب خصائص انتقال الحرارة القسري وانخفاض الظغط لمائع نانوي احادي الطبقة (كرافين-ماء) في انبوب دائري لجريان انسيابي وحمل حراري منتظم كشروط حدودية. اللزوجة والموصلية الحرارية للمائع (0.1-1wt%) النانوي تم قياسها.تأثير سرعة الجريان،الحمل الحراري وتركيز الجزيئات النانوية على تعزيز انتقال الحرارة تم تحريها.النتائج

بينت ان عدد نسلت للمائع النانوي (كرافين-ماء) يزداد بزيادة الحمل الحراري وسرعة الجريان.واعظم نسبة عدد نسلت (عدد نسلت مائع نانوي/عدد نسلتمائع اساسي) ومعامل الاداء الحراري كان (1.45) و(1.24) على التوالي، باستخدام تركيز (1wt%) وحمل حراري ($6104W/m_2$). واخيرا تحليل معامل الاداء يبين ان المائع الانوي كرافين يمكن ان يعمل كبديل جيد للموائع التقليدية في تطبيقات انتقال الحرارة.

الكلمات الرئيسية: انتقال الحرارة بالحمل، مائع نانوي كرافين، الجريان الانسيابي، انخفاض الضغط، معامل الاداء

1. INTRODUCTION

Most heat transfer applications use conventional fluids like ethylene glycol (EG), DI-water and engine oil as heat transfer working fluids. The efficiency of these fluids is often limited so the efficiency of the conventional fluids can be enhanced by improving the heat transfer properties and thermal conductivity. These heat transfer fluids have low thermal conductivity with respect to solid materials. Therefore, solid particles with high thermal conductivity are generally added to traditional heat transfer fluids to increase their thermal conductivity. However, the addition of micrometer or millimeter particles sized can cause problems as sedimentation and agglomeration. **Choi, 1995,** avoided these problems by introducing a new type of heat transfer medium referred to nanofluid where the nanoparticles are dispersed in base fluids like EG, water and oil.

A nanofluid is a new kind of heat transfer fluid prepared by dispersing metallic or non-metallic nanomaterials with typical size less than (100 nm) which are stably distributed in conventional fluids. These suspended nanomaterials in the liquid improve the thermal conductivity of conventional liquid. Nanofluids have been considered as innovative heat transfer fluids for numerous applications

The benefits of nanofluids technologies are expected to be large due to the heat transfer characteristic of cooling devices or heat exchangers in many applications. Nanofluids can show many advantages besides the abnormal high effective thermal conductivity. These advantages involve, **Murshed et al., 2008**: Reduction in pumping power, improving heat transfer and stability, miniaturizing systems, micro channel cooling without clogging and savings cost and energy.

Recently, several investigations were devoted to study of thermal properties such as thermal conductivity and viscosity as well as convective heat transfer characteristics of the nanoparticles based nanofluid prepared from different carbonic structures, like single-wall, multiwall carbon nanotubes, graphite nanoparticles, and diamond nanoparticles, graphene oxide, graphene. Among all of these structural forms, single layer graphene is a 2-D material with one carbon atom thickness layer was discovered **by Novoselov** in **2004**. It has unique thermal characteristics due to large specific surface area and high thermal conductivity compared with other carbonic forms. **Balandin, 2008,** reported values thermal conductivity single-layer graphene in-plane up to 5200W/mK which sounds impressive when compared to the axial thermal conductivity of carbon nanotubes, that is, 3000W/mK **,Chen, 2010**. Further, the thermal properties of graphene were expected to be much different from one dimension carbon nanotube and zero dimension nanoparticles. Because the graphene itself is a very good thermal conductor, so the graphene based nanofluid was normally expected to show important thermal conductivity improvement.

However, according to literature, theoretical and experimental studies on the heat transfer thermal properties such as viscosity and thermal conductivity as well as heat transfer improvement of graphene based nanofluids are scarce.

Rashidi, et al., 2014, studied experimentally the force convection heat transfer characteristics laminar flow of graphene nanosheets nanofluid through the shell and tube heat exchanger. The convective heat transfer coefficients of (GNP) graphene nanosheets based on water nanofluids under laminar conditions were measured. Also the effects of weight concentration and temperature on convective heat transfer coefficients of (GNP) graphene nanosheets nanofluid were discussed. Results of added 0.075wt% of (GNP) graphene nanosheets to the base fluid contributed to an improvement of thermal conductivity about 31.83% and the convective heat transfer coefficient up to 35.6% at 38 ºC compared with pure water.

Mehrali, 2015, investigated experimentally the heat transfer performances laminar forced convection for (GNP) nanofluid with 750m^2/g of specific surface area inside a circular tube under constant heat flux at different weight fraction concentrations (0.025-0.1wt.%). The effect of the nanoparticles concentration on thermal properties, thermal performance factor and convective heat transfer coefficient was examined. Thermal conductivity of GNP nanofluid enhancement from 12% to 28% was noticed compare to the base fluid. The heat transfer coefficient for the GNP nanofluid was found about 15% higher than the distilled water. The thermal performance factor for 0.1wt.% was found to be increased about 1.15.

Akhavan-Zanjani, et al., 2014, studied experimentally the convective heat transfer of graphene based water nanofluids in turbulent flow through a uniformly heated circular tube with various concentrations. Experiments were conducted to measure viscosity, thermal conductivity, heat transfer coefficient and pressure drop. Adding a small amount of nanoparticles led to moderate increment of viscosity and enhancement of thermal conductivity. Furthermore, heat transfer coefficient showed relatively high enhancement, and pressure drop remained without change. Results showed that the maximum augmentations were 4.95%, 6.04% and 10.30%, for viscosity, heat transfer coefficient and thermal conductivity, respectively.

The aim of this work is to investigate experimentally the effect of single layer of graphene DI-water nanofluid concentration on heat transfer enhancement and pressure drop through a circular tube under fully developed laminar flow and different uniform heat fluxes boundary conditions

2. EXPERIMENTAL APPARATUS AND PROCESS

The rig was built at convective heat transfer laboratory of **Texas A&M** University and it was composed of the following main parts and measuring apparatus. **Figs. 1** and **2** show the photo and schematic diagram of the experimental apparatus.

Copper pipe with length, inner and outer diameter of (90, 0.789, 0.9525) cm respectively is connected to the entrance length and other parts by polypropylene compression straight adapter to reduce the axial heat loss conduction as shown in **Fig. 3**. Nichrome wire is used to uniformly heat the copper pipe. The copper pipe is painted with a fine spray before the Nichrome wire is wrapped up around it to avoid electrical conduction. Five thermocouples (T-type) are soldered in the small cavity at the copper pipe surface before the heater wires are wrapped around it. Whole

copper pipe is enveloped with fiberglass insulation and aluminum tape to minimize heat losses to the surrounding.
Programmable (LAMBADA) Variable voltage and current transformer (0-600V, 0-2.6A) was used to adjust the input heater power as required. A variable speed magnetic pump (5-12V DC) is used to circulate the nanofluid inside the heat transfer loop. The pump is connected with variable voltage power supply to get desired speed.

An electromagnetic (Megameter) low flow from Seametrics (PE202 Megameter) is utilized to measure the velocity and volume flow rate of the working fluid flowing through the heat transfer rig. The accuracy of the measurement is +/- 1%. **Fig. 4** shows the electromagnetic flow meter.
An electromagnetic Wet/Wet Differential Pressure Transmitters (PX154) from Omega is used to measure the pressure drop of the working fluid across test section. The output of the pressure transmitter ranges from 4 to 20 mA. The accuracy of the pressure transmitter is +/- 0.75% of the full scale.
Nanofluid is purchased from (US Research Nanometarials, Inc USA) as single layer of graphene DI-water dispersion at weight fraction Concentration (1wt%) and to dilute it only add DI water and shake it up to desired concentration **Figs. 5** and **6** show a visual inspection of GNP nanofluids after 2 months of the nanofluid purchased. Although two months from preparation passed no sedimentation and agglomeration was observed.

The experiments include the study forced convection heat transfer performance and the pressure drop of a of single layer of Graphene DI-water nanofluid, with concentrations of (φ=1, 0.8, 0.6, 0.4, 0.2, 0.1 and 0 wt%) in plain tube. All the tests were carried out under fully developed laminar flow with mass flow rate of (0.36, 0.4, 0.468 0,526, 0.58, 0.65, 0.72) kg/min and uniform heat fluxes range (4292-6104 W/m^2).
Cleaning the test rig after finishing the readings for each concentration of the nanofluid is done by using the draining valve for preventing clogging and sedimentation.

3. EXPERIMENTAL CALCULATIONS

3.1 Heat Transfer Calculation

Comparisons of the Nusselt numbers at equal Reynolds number is unreliable and is uninteresting from a practical perspective. The comparison of nanofluids at the same Reynolds number is common in the literature for nanofluid fields. Based on many literatures, comparing the heat transfer at the same flow rates (pumping power) is considered a more appropriate method in a nanofluids study (**France,2010, Haghighi,2014 and Mehirli,2014**), therefore, the better choice is the constant velocity instead of constant Re number.

The actual heat flux is calculated from the two evaluations as follows:

1) The total amount of heat transfer created by the electrical heater is given as:

$$Q_1 = \zeta VI \quad (1)$$

where, I and V represent the current and voltage which generated by programmable power supply and pass through electrical heater as well as the factor ζ=0.97 represents the accounts of the heat lost to environment, **Akhavan-Behabadi, 2012**.

2) The amount of heat input is estimated from the sensible heat gained by the nanofluid as follow:

$$Q_2 = \dot{m}\, c_p\, (T_{out} - T_{in}) \quad (2)$$

where, T_{in} ,T_{out} , $\dot{m}$ and cp represent the temperature of the bulk fluid at inlet and outlet of the test section, mass flow rate and specific heat of working fluid respectively.

The actual heat flux is then estimated as follow:

$$q'' = \frac{0.5\,(Q1 + Q2)}{\pi d_o L} \quad (3)$$

The local heat transfer a characteristic was defined in terms of the Nusselt number Nu(x) and heat transfer coefficient h(x) as given below.

$$h(x) = \frac{q''}{(Tw - Tf)X} \quad (4)$$

$$Nu(x) = \frac{h(x)di}{k} \quad (5)$$

where T_f and T_w are the fluid and wall temperatures respectively, q" is the actual heat flux, k is the thermal conductivity of fluid, d_i is the inlet tube diameter and x is the axial distance from the test section inlet.

The temperature profile of fluid was obtained in the test section from the energy balance as follows:

$$T_{f(x)} = T_{f\,in} + \frac{q''Px}{\rho c_p u A} \quad (6)$$

Where P is the perimeter and A is cross-sectional area of the test section tube respectively, and u is the velocity of average fluid.

The average heat transfer coefficient and Nusselt number are calculated as follow:

$$h = \frac{q''}{(\bar{T}_w - \bar{T}_f)} \quad \text{and} \quad Nu = \frac{hd}{k}$$

Here, $\bar{T}_w$ is the average temperature of the wall and $\bar{T}_f$ is the average bulk temperature of fluid.

Specific heat capacity and density of nanofluids are calculated from:

$$C_p=\frac{q''}{\dot{m}(T_{in}-T_{out})} \quad (7)$$

$$(\rho C_p)_{nf}=\varphi(\rho C_p)_p+(1-\varphi)(\rho C_p)_f \quad (8)$$

3.2 Friction Factor Calculation

Friction factor based on practically measured pressure drop can be evaluated by using Darcy friction factor equation, **Frank, 2001**.

$$f=\frac{\Delta P}{(\rho u^2/2)}\frac{d}{L} \quad (9)$$

Where Δp is the pressure drop through the test section measured by using an electromagnetic pressure transducer.

4. MEASURMENT OF VISCOSITY AND THERMAL CONDUCTIVITY

The viscosity of the GNPs based DI-water nanofluids at different weight fractions concentrations (1, 0.9, 0.8, 0.7, 0.6, 0.5, 0.4, 0.3, 0.2 and 0.1wt%) were measured by using a rotational type low viscosity DV-I prime digital viscometer. Measurements are taken at different shear rates and temperatures range from (5, 10, 15, 20, 25, 30 and 35°C) and were repeated four times for each experiment to obtain an accurate results.

Thermal conductivity of GNPs based DI-water nanofluids with six various weight fraction concentrations (1, 0.8, 0.6, 0.4, 0.2, 0.1 wt%) at temperatures range from (5-35ºC) is measured by using a KD2 Pro instrument from (Decagon devices, Inc. USA). The measurements were taken under different temperature conditions by using a temperature-controlled container connected with chiller to maintain constant temperature of sample.

5. RESULTS AND DISCUSSION

At first the experiments were conducted for DI- water. The results of experiments for DI-water under constant and uniform heat flux condition were compared with the data from the traditional standard equations, like the Shah and Darcy equations for laminar flow **Jang, 2009** as flowing:

$$Nu=\begin{cases}1.302x_*^{-\frac{1}{3}}-1 & x_*\le 0.00005\\ 1.302x_*^{-\frac{1}{3}}-5 & 0.00005\le x_*\le 0.0015\\ 4.346+8.68\left(10^3\,x_*\right)^{-0.506}\exp\left(-41x_*\right) & x_*\ge 0.001\end{cases} \quad (10)$$

where

$$Nu_* = h(x)d_i/k$$

$$x_* = \left[\frac{\frac{x}{di}}{RePr}\right]$$

$$f = \frac{64}{Re} \quad (11)$$

Fig. 7 illustrates the comparison between the average Nusselt number from experiments results and the results from Shah Equation. Data from this classical correlations and the experimental Nusselt number for DI- water agrees well and shows the precision of the experimental-setup with an error rate of less than 1.5%. To verify the friction factor data, **Fig. 8** shows the friction loss validation for DI-water from the experimental study, and the Darcy equation with an error rate of less than 3%.

Fig.9 shows reduction in the viscosity of the DI-water and GNPs nanofluid when the temperature is increasing. This is due to that, when the temperature is rising that causes the weakening of the adhesion forces for inter-particles intermolecular and that reducing the average forces of intermolecular. Subsequently, the viscosity reduces when the temperature increases that which noticed for the most kinds of nanofluids as shown in previous work**. Fig. 10** shows the maximum increment in viscosity of GNPs based DI-water is 111% at 1 wt% weight concentration and temperature 35 ºC compared with base fluid.
Thermal conductivity of the GNPs nanofluids with various weight fraction concentrations and temperature ranging from (5 to 35°C) are shown in **Fig. 11**. It is clear from this figure that the thermal conductivity enhancement was obtained with increasing weight concentrations and temperature. **Fig. 12** shows the thermal conductivity enhancement ratio. The maximum enhancement ratio in thermal conductivity for 1 wt% of GNPs was 22% at 35 ºC and 10% for 0. 1 wt % concentration was compared with base fluid.

Figs. 13, 14 and **15** reveal the variation of the average Nusselt number with velocity flow rate for GNPs nanofluid in a plain tube at different weight fraction concentrations (0.1-1wt%) and heat fluxes of 6104, 5040 and 4292W/m^2, respectively. The Nusselt numbers were largely influenced by the thermophysical properties (viscosity and thermal conductivity), the Brownian motion of nanoparticles, and the specific surface area of the nanoparticles. Therefore, the high concentration, heat flux, and nanofluid velocity causes an increase in the values of the Nusselt number. The enhanced heat convection performance of the GNPs nanofluid was resulted from the disordered movement of the nanoparticles and the high thermal conductivity of the GNPs nanofluid. As the nanoparticles concentration and fluid velocity increase the Nusselt number increases because the effective thermal conductivity of GNPs nanofluid increases with increasing weight concentration of the nanoparticles, which is explained by Brownian motion of the nanoparticles, molecular-level layering of the liquid at particle/liquid interface. Improved thermal conductivity reduces resistance to thermal diffusion in the laminar sublayer of boundary layer.

From figures, it can be seen that, the largest enhancement of the Nusselt number were 17.9%, 22.19%, 28.16%, 32.5%, 39.6% and 45.28% for the φ_m= 0.1, 0.2, 0.4, 0.6, 0.8 and 1wt %, respectively at a heat flux of 6104 W/m^2.

The augmentation in the heat transfer (the Nusselt number ratio) ($Nu_{nanofluid}/Nu_{plain\ tube}$) is shown in **Figs. 16, 17** and **18**. The maximum enhancement in the heat transfer for GNPs was (1.528) at velocity (0.25 m/s) heat flux (6104 W/m^2) and concentration (1wt%).

Fig. 19 shows the Nusselt number at different heat fluxes for the (1wt %) GNPs nanofluids. The Nusselt number had an enhancement of 33.9%, 40.9%, and 45.2% for the heat fluxes of 4292, 5040, and 6104 W/m^2, respectively.

The improvement in heat transfer coefficient in nanofluid is attributed to the effective thermal conductivity of nanofluid solution. The heat transfer coefficient is given as (k/δt), where (δt) is the thermal boundary layer thickness. This means that the decreasing thermal boundary layer thickness and/or improvement of nanofluid thermal conductivity increases the heat transfer coefficient and lead to increase the Nusselt number. Also, it seems that, the thermal boundary layer thickness of nanofluids is less than that of the DI-water. Furthermore, the thermal dispersion contributes to this improvement is because of the inherent irregular and random motion of graphene nanoparticles. Therefore, the temperature gradient at the wall becomes steeper, and that cause increasing in heat transfer rate.

The variation in friction factor at different velocities and weight fraction concentrations for GNPs nanofluid for plain tube is shown in **Fig. 20**.
Fig. 21 shows the effect of different studied parameters on friction factor ratio ($f_{nanofluid}/f_{plain\ tube}$). Maximum increase in ($f_{nanofluid}/f_{plain\ tube}$) for GNPs nanofluid was (1.74) at velocity flow rate of (0.25 m/s) and concentration of (1wt%).
The thermal performance factor of the GNPs nanofluid can be used to determine the usefulness of GNPs nanofluids for application in thermal systems.

$$\eta = \left(\frac{Nu_{nf}}{Nu_{bf}}\right) / \left(\frac{f_{nf}}{f_{bf}}\right)^{1/3} \quad (12)$$

The results showed that the thermal performance factor of the GNPs nanofluid is high at a high heat flux and increased as the velocity and heat flux increased as shown in **Figs. 22, 23** and **24**. This is a result of the superior efficiency of the fluid disturbance and thus the heat transfer caused by the high values of thermal conductivity at the same pumping power. The maximum thermal performance of the GNPs nanofluid increased up to 1.25, 1.22, and 1.18 for 1 wt % of GNPs nanofluid at heat fluxes of 6104, 5040, and 4292W/m^2, respectively as shown in **Fig. 25.** Finally, an analysis of the pressure drop and the heat transfer result via the thermal performance factor shows that in spite of the pressure losses and the pumping power penalty, the GNPs based DI-water nanofluid is an excellent alternative for traditional working thermal fluids in heat transfer applications.

Nusselt number and friction factor can be related with Reynold number, Re, Prandel number, Pr, and nanofluid weight concentration, φm, with GNPs based DI-water nanofluids through the following correlations:

$$Nu=a_1 Re^{a_2} Pr^{a_3} (1+\varphi_m)^{a_4} \quad (13)$$

The limitations for this correlation are (Re=563-2158), (Pr=6.1-11.3) and nanofluid concentration (φ_m=0.1-1 wt%). The value of constants and the deviations are given in **Table 2.**

$$f=b_1 Re^{b_2} (1+\varphi_m)^{b_3} \quad (14)$$

The limitations for this correlation are (Re=563-2158), (Pr=6.1-11.3) and nanofluid concentration (φ_m=0.1-1 wt%).The value of constants and the deviations are given in **Table 3**.

Figs. 26 and **27** give the representation of the above correlations.

The comparison of the present experimental results of GNPs based water nanofluid with the published work, of **Mehrali, 2015**, is shown in **Fig. 28** for Nusselt number. This comparison shows a reasonable agreement with an error not exceeds 17%.

6. CONCLUSIONS

The following conclusions were obtained:

1. Thermal conductivity enhances as the nanofluid temperature and concentrations increase, and maximum enhancements was around 11.9% to 22.2% with weight concentration of 1wt % and temperature range from 5 to 35ºC.

2. Viscosity of the GNPs nanofluid was dependent on the concentration and temperature. It decreases with increases the temperature, and their increment was 80−111% of 1wt % compared with DI-water when the temperature increased from 5 to 35 ºC.

3. The Nusselt number enhances as the heat flux and velocity flow rate increase and maximum Nusselt number ratio ($Nu_{nanofluid}/ Nu_{plain\ tube}$) was (1.45) by using (1wt%) GNPs based DI-water nanofluid and the maximum thermal performance factor was (1.24). The GNPs nanofluid provides a good choice for the replacement of the traditional working fluids in heat transfer applications.

REFERENCE

- Akhavan-Behabadi M.A., Saeedinia M. and Nasr M.,2012 *"Experimental study on heat transfer and pressure drop of nanofluid flow in a horizontal coiled wire inserted tube under constant heat flux"*, Experimental Thermal and Fluid Science Vol.36, P.158–168.
- Akhavan-Zanjani, 2014, *Turbulent Convective Heat Transfer and Pressure Drop of Graphene–Water Nanofluid Flowing inside aHorizontal Circular Tube*, Journal of Dispersion Science and Technology,35 P. 1230–1240.

- Balandin A., Ghosh S., Bao W., Calizo I. and Teweldebrhan D.,2008, "*Superior Thermal Conductivity of Single-Layer Graphene"*, Nano Letters Vol.8, P.902-907.
- Chen L. and Xie H.,2010, "*Surfactant-Free Nanofluids Containing Double- and Single-Walled Carbon Nanotubes Functionalized by a Wet-Mechanochemical Reaction"*, Thermochim. Acta Vol.497, P.67–71.
- Choi S. and Eastman A.,1995,*"Enhancing thermal conductivity of fluid with nanoparticles"* , in: D.A. Siginer, Developments and Applications of Non-Newtonian Flows, Vol.66, P.99–105.
- France, Timofeeva E. and Singh, D.,2010,*"Thermophysical property-related comparison criteria for nanofluid heat transfer enhancement in turbulent flow"* Appl. Phys. Lett., Vol.96(21), P.213109.
- Frank M, White,2001,*"Fluid Mechanics"*, Fourth edition, MacGraw-Hill books.
- Jang S., Hwang K. and Choi U.,2009, *Flow and Convective Heat Transfer Characteristics of Water-Based Al2O3 Nanofluids in Fully Developed Laminar Flow Regime*, International Journal of Heat and Mass Transfer Vol.52, P.193–199.
- Haghighi E., Saleemi, M., Muhammed, M. and Palm B.,2014,*"Accurate basis of comparison for convective heat transfer in nanofluids"*, International Communications in Heat Mass Transfer, Vol.52, P.1−7.
- Murshed S.M.S, Leong K.C. and Yang C.,2008,*"Thermophysical and electrokinetic properties of nanofluids" – A critical review*, Vol.28, P.2109-2125.
- Mehrali M., Sadeghinezhad E. and Rose A.,2015,"*Heat Transfer and Entropy Generation for Laminar Forced Convection Flow of Graphene Nanoplateletsnano fluids in a Horizontal Tube"*, International Commun. in Heat and Mass Transfer Vol.66, P.23-31.
- Mehrali M.,Sadeghinezhad E., Mehrali M. and KaziS. N.,2014,*"Experimental investigation of convective heat transfer using graphene nanoplatelet based nanofluids under turbulent flow conditions"*, Industrial & Engineering Chemistry Research, Vol.53, P.12455−12465.
- Novoselov K., Geim A., Morozov S., Dubonos S. and Firsov A.,2004,*"Electric field effect in atomically thin carbon films"*, Science Vol.306, P. 666.

- Rashidi A.,Ghozatloo A. and Shariaty-Niassar M.,2014,"*Convective Heat Transfer Enhancement of Graphene Nanofluids in Shell and Tube Heat Exchanger"*, Experimental Thermal and Fluid Science Vol.53, P.136–141.

NOMENCLATURE

ρ= density, kg/m^3

f= friction factor

nf= Nanofluid

bf= Base fluid

η= thermal performance factor

φ_m= mass or weight friction concentration

Q_1=total heat power, W/m^2

Q_2=sensible heat gained by the nanofluid,W/m^2

P¯=perimeter, m

u= velocity, m/s

I=current,omh

V=voltage,Volt

T=temperature, ˚C

L= length of tese section, m

$\dot{m}$=mass flow rate,kg/s

q"=actual heat flux,W/m^2

ζ= factor of heat loss to ambient

d= diameter, m

Cp= specific heat, KJ/kg.K

h= heat transfer coefficient, W/m^2.k

Table 1. Graphene nanoparticles properties.

Properties	Specifications
Color	black liquid
Shape of particle	single layer nanoplatelets
Content of carbon	>99.3 wt%
Surface area	500 - 1200m^2/g
Bulk density	0.2–0.4 g/cm3
diameter of particle	1μm - 12μm
Thickness of particle	0.55nm - 1.2nm
Thermal conductivity (vertical to surface)	6 W/m K
Thermal conductivity (parallel to surface)	5000 W/m K

Table 2. Values of factors for Eq.(13).

Nanofluid	a_1	a_2	a_3	a_4	a_5	Deviation
GNPs DI-water	0.6451	0.4180	-0.3730	6.9672	0	± 7.5%

Table 3. Values of factors for Eq.(14).

Nanofluid	b_1	b_2	b_3	b_4	Deviation
GNPs DI-water	54.450	-0.9752	-2.2072	0	± 10.5%

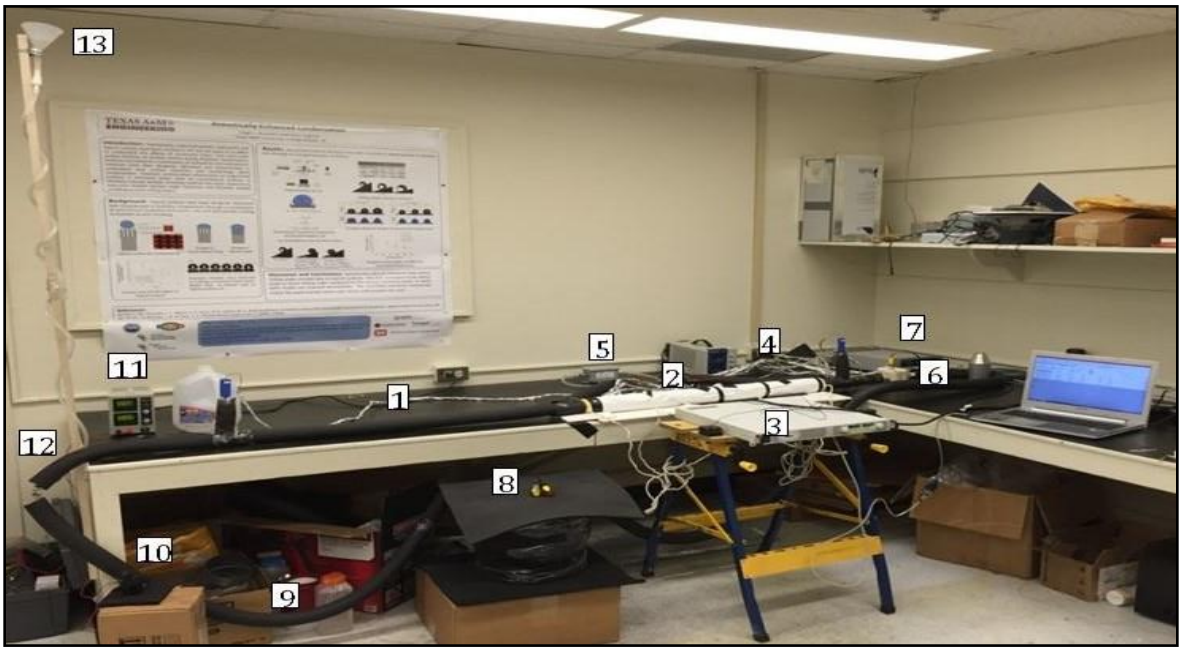

Figure 1. Heat Transfer loop at convective laboratory.

1. Entrance length **2.** Test section **3.**Variable voltage transformer **4.** Thermocouples **5.** Pressure transducer **6.** Flow meter **7.** Data acquisition system **8.** Heat exchanger **9.** Silicone Rubber Tubing **10.** Pump **11.** Power supply **12.** Control valve **13.** Plastic funnel

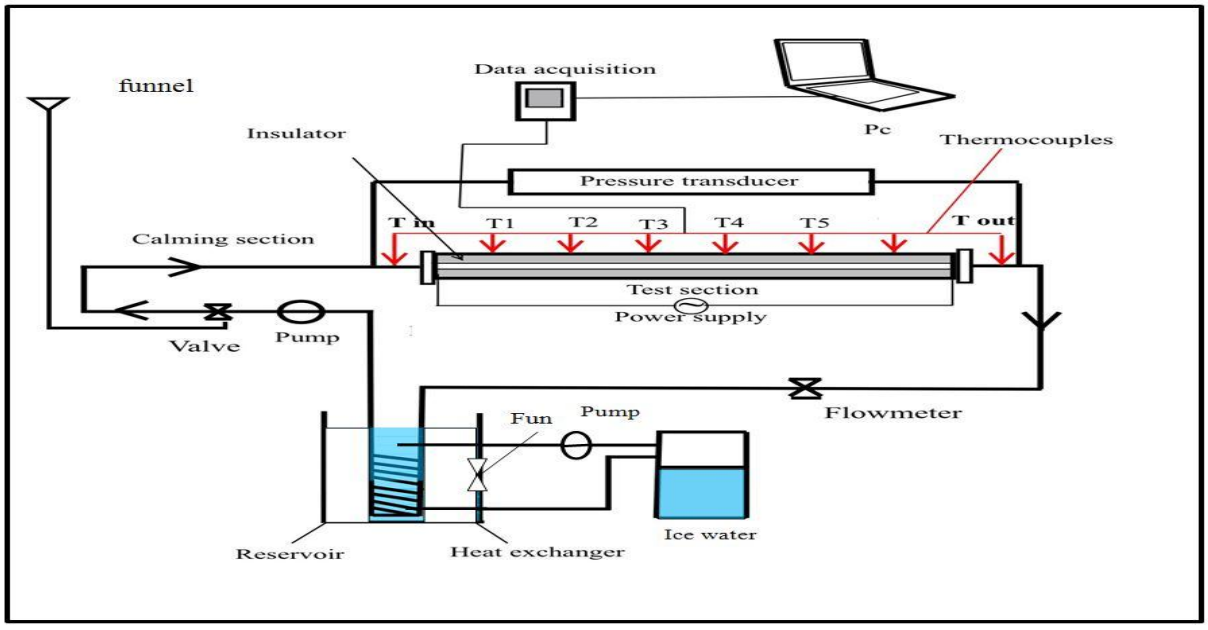

Figure 2. Schematic diagram of experimental apparatus.

Figure 3. Polypropylene compression straight adapter to reduce the axial heat loss conduction.

Figure 5. Nanofluid samples.

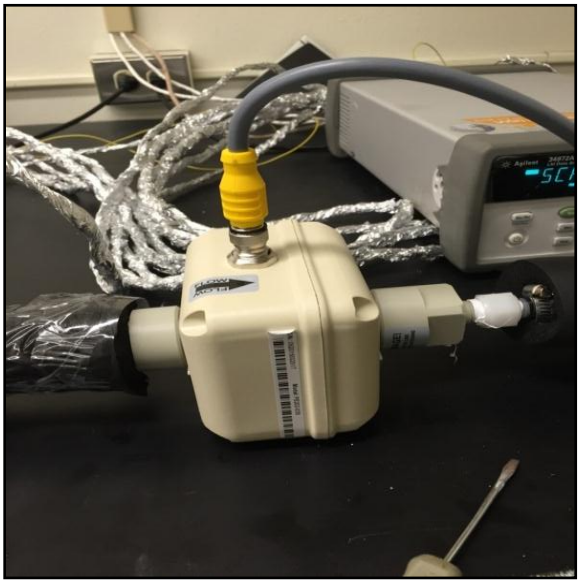

Figure 4. Electromagnetic flow meter.

Figure 6. Nanofluid samples after two months.

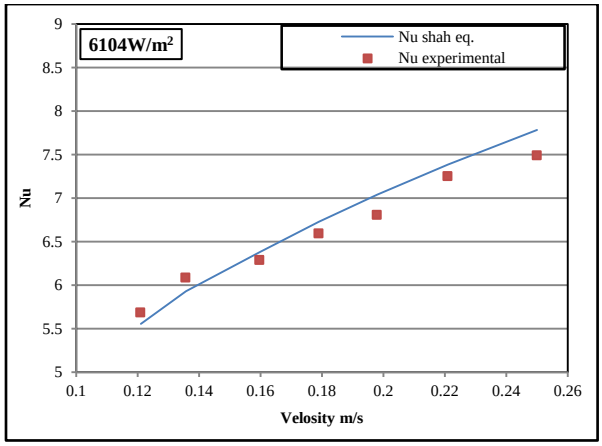

Figure 7. Measured average Nusselt number and the prediction correlations for DI-water versus the velocity.

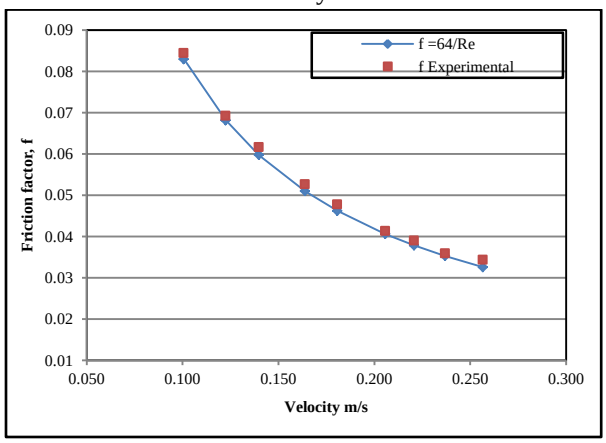

Figure 8. Frictional head loss as a function of the velocity for DI-water.

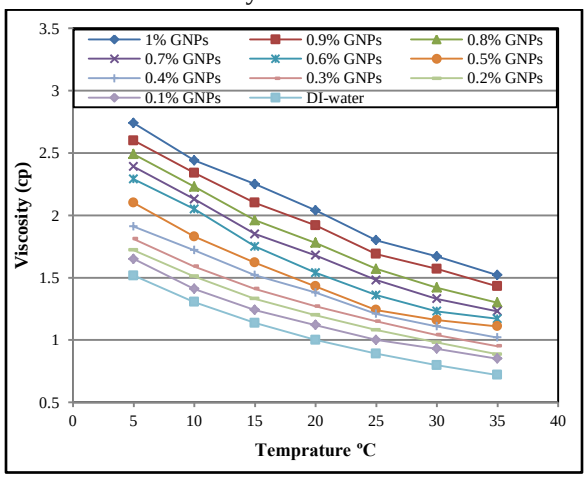

Figure 9. Viscosity of GNPs nanofluid with different weight fraction concentrations.

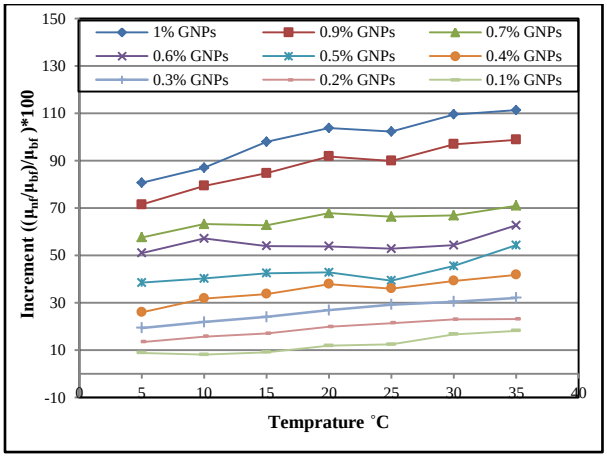

Figure 10. Viscosity of GNPs nanofluid increment percentage compared with DI-water.

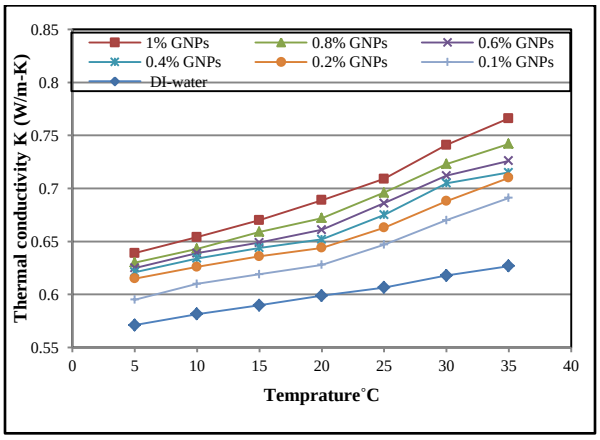

Figure 11. Thermal conductivity of GNPs with different weight concentrations.

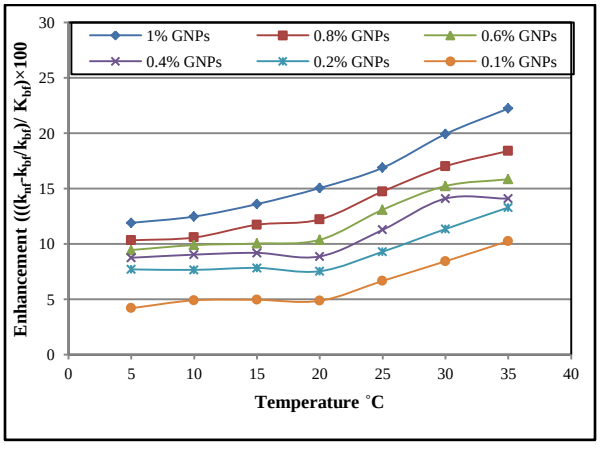

Figure 12. Thermal conductivity enhancement percentage compared with DI-water.

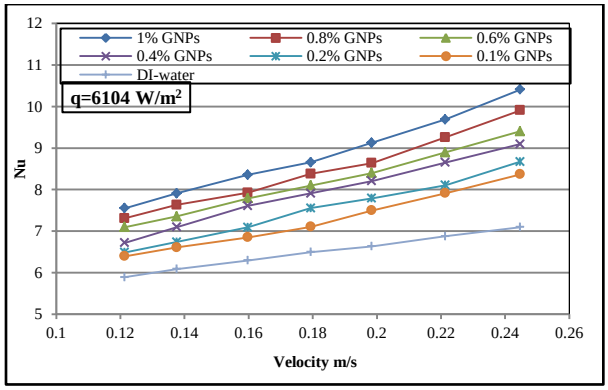

Figure 13. Effect of velocity of GNPs nanofluid on Nusselt number for different weight concentrations at q=6104 W/m^2.

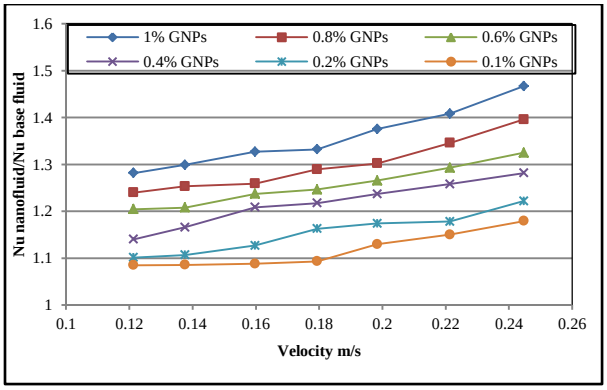

Figure 16. Effect of velocity of GNPs nanofluid on Nusselt number ratio (Nu $_{nanpfluid}$/Nu $_{DI-water}$)for different weight concentrations at q=6104 W/m^2.

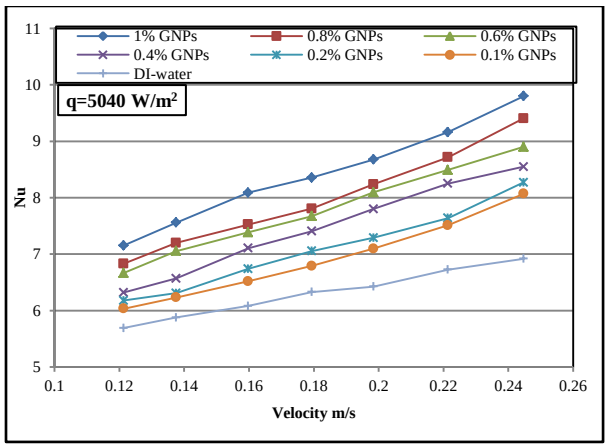

Figure 14. Effect of velocity of GNPs nanofluid on Nusselt number for different weight concentrations at q=5040 W/m^2.

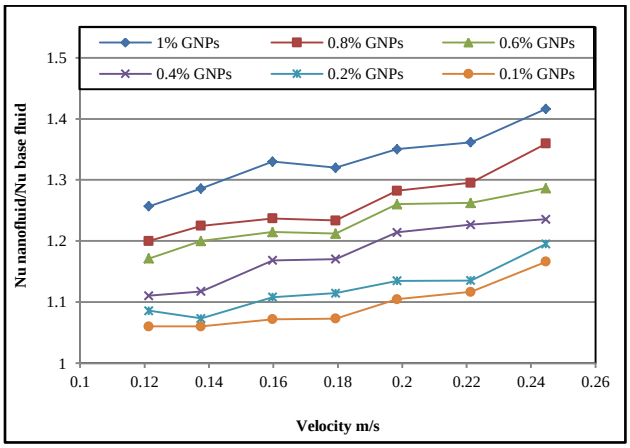

Figure 17. Effect of velocity of GNPs nanofluid on Nusselt number ratio (Nu $_{nanofluid}$/Nu $_{DI-water}$)for different weight concentrations at (q=5040 W/m^2).

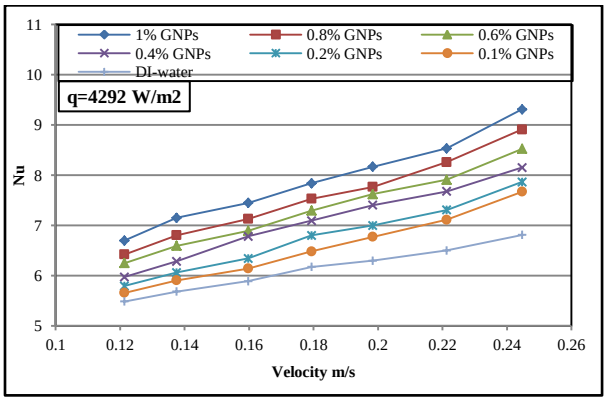

Figure 15. Effect of velocity of GNPs nanofluid on Nusselt number for different weight concentrations at q=4292 W/m^2.

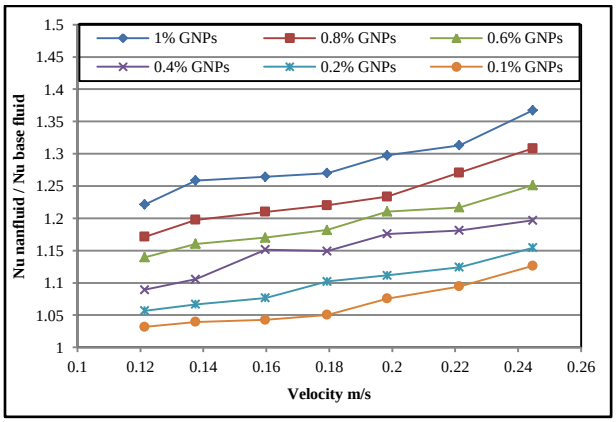

Figure 18. Effect of velocity of GNPs nanofluid on Nusselt number ratio (Nu $_{nanpfluid}$/Nu $_{DI-water}$)for different weight concentrations at q=4292 W/m^2.

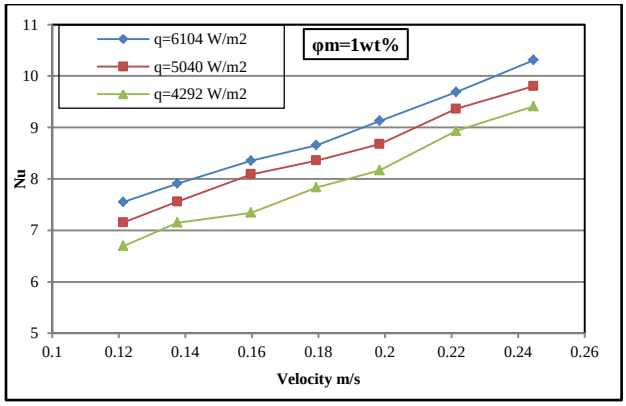

Figure 19. Effect of heat flux on Nusselt number for GNPs nanofluid for different weight concentrations.

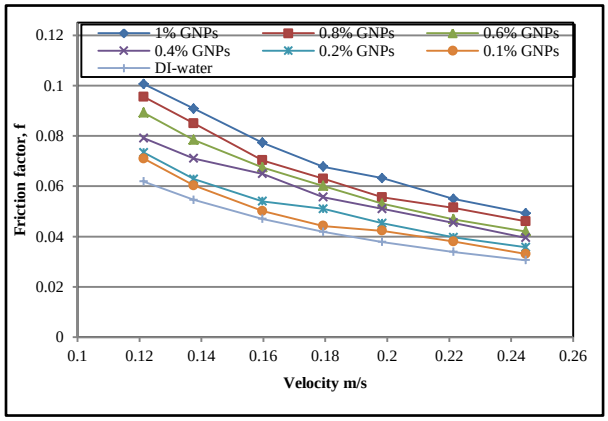

Figure 20. Variation of friction factor at different velocities and weight concentrations for GNPs nanofluid.

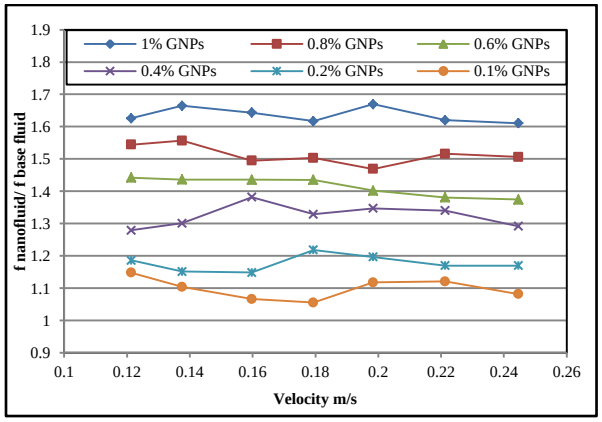

Figure 21. Variation of friction factor ratio ($f_{nanofluid}$/ $f_{plain\ tube}$) at different velocities and weight concentrations for GNPs.

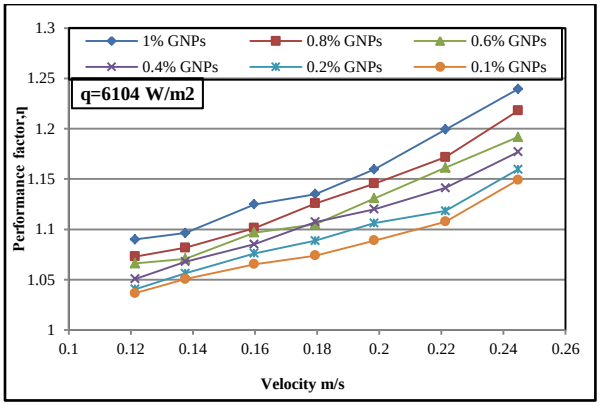

Figure 22. Effect of velocity and concentration on performance factor (η) for GNPs nanofluid at q=6104 W/m^2.

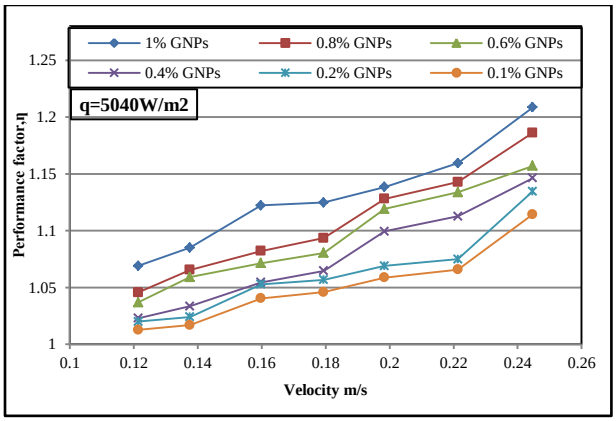

Figure 23. Effect of velocity and weight concentration on performance factor (η) for GNPs nanofluid at q=5040 W/m^2.

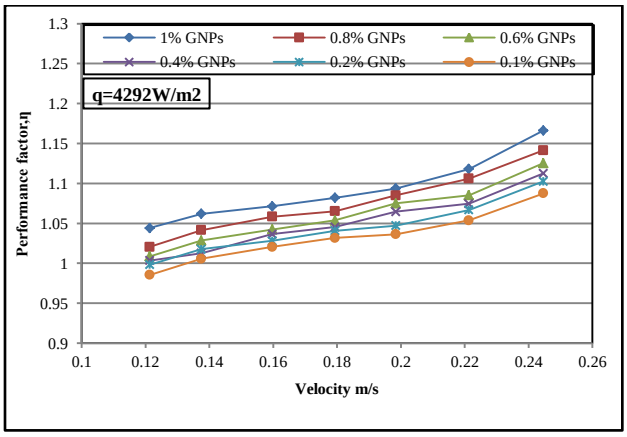

Figure 24. Effect of velocity and weight concentration on performance factor (η) for GNPs nanofluid at q=4292 W/m^2.

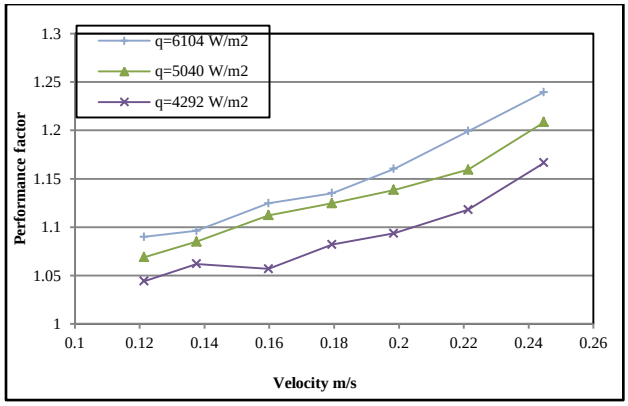

Figure 25. Effect of velocity on performance factor (η) for (1wt%) concentration of GNPs nanofluid at different heat flux.

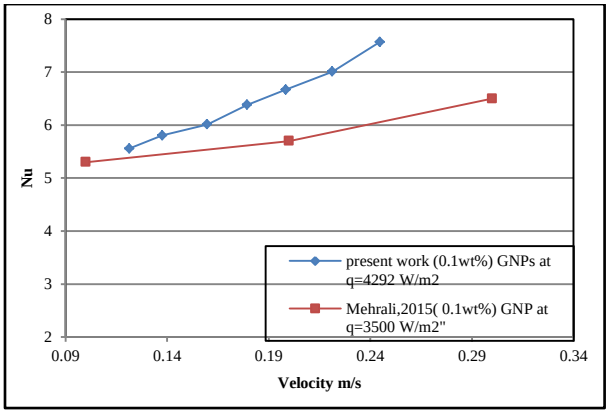

Figure 28. Comparison of experimental result of Nusselt number for present work with the published data of **Mehrali, 2015**.

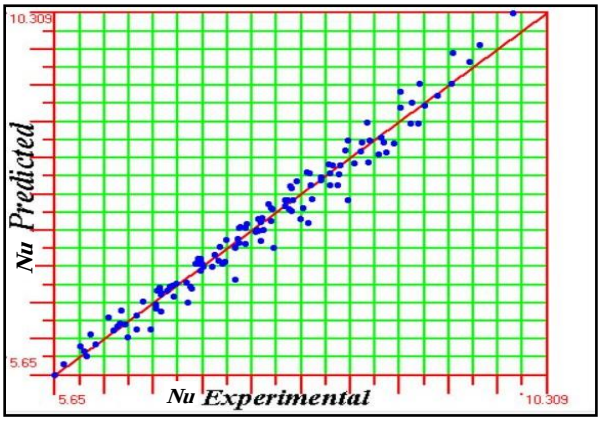

Figure 26. Comparison of experimental data with regression equation of Nusselt number for GNPs nanofluid.

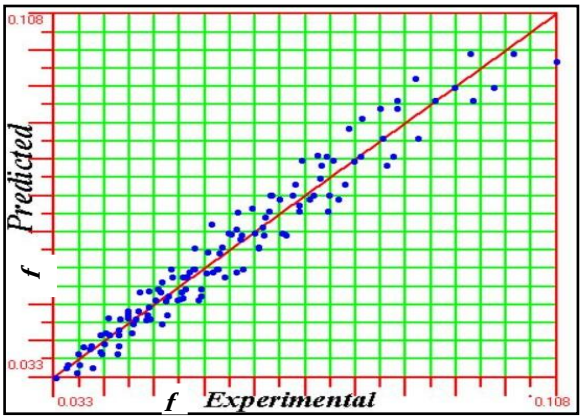

Figure 27. Comparison of experimental data with regression equation of friction factor for GNPs nanofluid.